

# Time-reversal focusing of elastic surface waves

Pelham D. Norville<sup>a)</sup> and Waymond R. Scott, Jr.<sup>b)</sup>

*School of Electrical and Computer Engineering, Georgia Institute of Technology, Atlanta, Georgia 30332*

(Received 3 December 2004; revised 7 April 2005; accepted 6 May 2005)

Time-reversal focusing is experimentally applied in an elastic medium in the presence of multiple scattering objects on the order of a wavelength in size. The effectiveness of time-reversal is compared to time-delayed focusing and uniform excitation of the transducer array for focusing energy to a desired location within the medium. A filter is also designed to improve the bandwidth of the excitation signal. Time-reversal focusing is investigated in the context of an elastic-wave landmine detection system. Results are presented demonstrating the advantages and limitations of time-reversal in excitation of a resonance in a TS-50 landmine buried in the medium. A special case is presented for a landmine buried in shadow regions where uniform excitation fails to illuminate the target while time-reversal focusing yields improved target illumination. © 2005 Acoustical Society of America. [DOI: 10.1121/1.1945468]

PACS number(s): 43.35.Pt, 43.20.El, 43.20.Fn, 43.20.Tb [PEB]

Pages: 735–744

## I. INTRODUCTION

A landmine detection system (Fig. 1) is under development at the Georgia Institute of Technology that functions by exciting elastic waves that propagate through the soil.<sup>1</sup> A feature of this system is a noncontact sensor that is used to measure ground motion, making it possible to sense motion directly above a landmine. While multiple wave types are generated by the system's excitation signal, the wave of primary importance in detecting landmines is the Rayleigh surface wave. This wave propagates near the surface along the boundary between the air and the soil and interacts with objects buried in the medium. For most objects, this interaction is observed as scattering of the Rayleigh wave front off of the object. When the buried object is a landmine, due to its structure, and the depth at which it is usually buried, the Rayleigh wave may excite a resonance in the layer of soil between the surface and the flexible top of a landmine. This resonance enhances the surface displacements and is the primary detection cue for buried landmines.<sup>1</sup>

Scattering off clutter objects in the medium causes the Rayleigh wave to become disorganized. If a large number of objects are present, the scattering can interfere with the Rayleigh wave to the point that it no longer effectively illuminates the buried landmine. Any resonance that is excited will be difficult to detect in the presence of the numerous scattered waves reflecting off objects in the medium. By applying time-reversal focusing methods to seismic detection techniques, energy can be focused to a specific location within the medium, irrespective of the presence of clutter. This allows one to focus energy to a certain spot in order to excite a resonance in any target that may be present there.

The primary experimental and numerical investigations of time-reversal focusing have been in the ultrasound frequency range and in the far field.<sup>2–4</sup> Time-reversal focusing

has been investigated in both fluid and solid media, including liquid-solid interfaces. In fluid media, homogeneous backgrounds have been augmented with scattering objects to create high order scattering of incident waves.<sup>5</sup> In these scenarios, time-reversal focusing has been shown to be effective in inhomogeneous media,<sup>6</sup> even producing super-resolution effects in some cases.<sup>5,7,8</sup> In solid media, inhomogeneity from microstructural defects has been examined. These experimental investigations form a solid foundation in the exploration of time-reversal focusing, but the experimental cases that have been examined are still significantly different from those encountered in the landmine or buried target detection problem.

The research presented in this paper considers the effectiveness of time-reversal in the significantly different problem of seismic buried object detection.<sup>9</sup> In this detection problem, sources are in the near field, only a few wavelengths from the targets and scattering objects. The number of scattering objects per unit area is also significantly less than in previously considered scenarios.<sup>6,10,11</sup> The seismic system differs significantly from ultrasound systems in that energy is coupled directly into the soil, rather than through a fluid. The coupling of the transducer motion into the soil significantly alters the frequency response of the excited wave.

This paper first presents the basic theory of time-reversal focusing with respect to its application to elastic media. This is followed by a description of the method used to implement elastic wave time-reversal focusing in a laboratory at the Georgia Institute of Technology. This description will include a discussion of the experimental facility and the measurement techniques. The design of a filter used to improve the bandwidth of the excitation signals is also presented. Results from several experiments are shown and analyzed. An ensuing evaluation of the experimental results demonstrates the effectiveness as well as the limitations of time-reversal focusing in buried object detection.

<sup>a)</sup>Electronic mail: norville@ece.gatech.edu

<sup>b)</sup>Electronic mail: waymond.scott@ece.gatech.edu

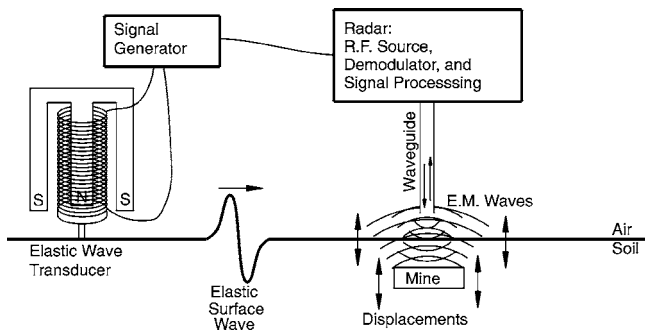


FIG. 1. Schematic of the elastic wave landmine detection system.

## II. BASIC TIME-REVERSAL THEORY

The governing wave equation for elastic waves in solids serves as the starting point for a basic analysis of time-reversal,

$$\rho_s \frac{\partial^2 \mathbf{u}}{\partial t^2} = (\lambda + 2\mu)(\nabla(\nabla \cdot \mathbf{u})) - \mu(\nabla \times (\nabla \times \mathbf{u})), \quad (1)$$

where  $\mathbf{u}$  is displacement,  $\lambda$  and  $\mu$  are the Lamé constants of the medium and  $\rho_s$  is the density.

This equation is valid for the case for which there are no external forces (body forces) present on the medium. It also assumes that the medium is lossless with respect to wave propagation. The assumption of a lossless medium is not physical, but if the losses are very small, the additional terms in the equation have a negligible effect and can be ignored.

An examination of the wave equation shows that there are only second-order time derivatives present. Because of the lack of odd-order time derivatives, if there is a solution to this equation  $\mathbf{u}(\mathbf{r}, t)$ , then  $\mathbf{u}(\mathbf{r}, -t)$  must also be a solution to this equation. Because experimentally it is necessary to work with reverse time in a causal fashion, a finite time duration must be selected over which the equation will be considered. The formulation  $\mathbf{u}(\mathbf{r}, T-t)$  over the interval  $(T, 0)$  satisfies the causality requirement. If all energy in the spatial region of interest is small outside of this time interval, then this solution should be almost exactly equal to  $\mathbf{u}(\mathbf{r}, -t)$ .

A time-reversal cavity is a three-dimensional (3D) surface which is constructed around a location of interest, usually a source location. All waves impinging on this surface are recorded, time-reversed, and re-transmitted. Classical time-reversal focusing further simplifies this to a time-reversal mirror (TRM) where only a portion of the time-reversal cavity is realized. The TRM concept is well documented in the literature.<sup>6</sup>

In the case of elastic surface waves, the principle wave mode of interest is the Rayleigh wave, a surface wave that decays exponentially with depth. Though some energy is lost from mode conversion and from scattering objects in the soil, most of the Rayleigh wave's energy remains near the surface. Given that landmines are buried near the surface and the energy in the Rayleigh wave is concentrated in that region, the landmine detection problem is approached here as a quasi-two-dimensional problem.

To construct a TRM, receivers are realized as a simple array. The array subtends some angle of the 3D surface that



FIG. 2. (Color online) Geometry of the implementation of time-reversal focusing.

would be necessary to surround the focus point. This array is much more practical to implement than a time-reversal cavity, but it is subject to the limitations of array techniques. The number and spacing of the array elements will have effects on grating lobes. The spot size of the focus point is also limited by the TRM aperture and diffraction effects proportional to wavelength.<sup>2</sup> The TRM concept has been verified in the ultrasound regime for fluid and elastic media.<sup>10,12</sup>

## III. THE TIME-REVERSAL FOCUSING METHOD

### A. Implementation

For the experimental implementation of time-reversal focusing, elastic wave sources are located in an array  $S_n = (x_{S_n}, y_{S_n} | n=1, 2, \dots, N)$  (Fig. 2). First, consider the effect of time-reversal from a single source,  $S_n$ .

**Step 1:** Transmit an excitation signal,  $\epsilon(t)$ , from source  $S_n$ .

**Step 2:** Receive a signal,  $f_n(t)$ , at the desired focusing location,  $R$ . Propagation through the medium is described by a Greens function,  $G(S_n, R, t)$  such that

$$f_n(t) = \epsilon(t) * G(S_n, R, t). \quad (2)$$

**Step 3:** Time-reverse the received signal:  $f(t) \Rightarrow f(-t)$ .

**Step 4:** Transmit the time-reversed signal,  $f(-t)$ , from  $S_n$  and record at any location on the surface,  $\mathbf{r}$ , such that the signal recorded at  $\mathbf{r}$  is

$$U_n(\mathbf{r}, t) = [\epsilon(-t) * G(S_n, R, -t)] * G(S_n, \mathbf{r}, t). \quad (3)$$

Recalling the associative property of convolution,  $U_n(\mathbf{r}, t)$  then is the cross correlation of the two Greens functions convolved with the time-reversed excitation function,  $\epsilon(-t)$ . In the special case when  $\mathbf{r} = R$ , this becomes the auto-correlation function. This yields a mathematical explanation for the observed focusing of the signal that occurs at  $R$ .

This process can be extended to include additional transmitters in the array such that

$$U(\mathbf{r}, t) = \sum_{n=1}^N [\epsilon(-t) * G(S_n, R, -t)] * G(S_n, \mathbf{r}, t). \quad (4)$$

In the experimental implementation of this method, **steps 1–3** are performed once for each transmitter  $S_n$  in the

array. **Step 4** is performed simultaneously for all transmitters  $S_{1...N}$ .

Traditional time-reversal focusing using a TRM requires that either a source be located at the desired focus location ( $R$ ) or that an excitation be launched from the transducer array. In the latter case, after the excitation is launched from the transducer array, reflections off a target at the focal location act as a passive source. These reflections are recorded at the TRM, time-reversed, and retransmitted. In the landmine or buried target detection problem, the signal reflected off a target is not strong enough to be significantly above the noise floor. This makes it impractical to use reflected signals as a source for time-reversal focusing. Further, in the case of landmine detection, it would be unwise to place a seismic source at a location where a landmine is believed to be buried.

While the time-reversal focusing method used in the experiments presented in this paper (Fig. 2) is similar to the concept of a TRM, there is noteworthy difference. A TRM relies on reciprocity of the propagation from the source to the focus point,  $G_n(R, S_n, t) = G_n(S_n, R, t)$ . Applying reciprocity to  $U(\mathbf{r}, t)$  will yield the autocorrelation function for the case of  $\mathbf{r} = R$ . In the case of an anisotropic propagation medium, reciprocity may not be valid, and traditional TRM implementation could fail to yield the autocorrelation function for the special case of  $\mathbf{r} = R$ .

## B. Excitation methods

To investigate the relative effectiveness of time-reversal focusing in elastic media, time-reversal excitation methods will be compared to time-delay focusing methods. Uniform excitation of the transducer array will also be used to serve as a baseline measurement to demonstrate the improvement of each focusing method over a non-focused excitation method.

The results are presented with respect to a differentiated Gaussian pulse excitation [Eqs. (5) and (6)], with center frequency,  $\omega_c$ , and time delay,  $t_d$ . For collection of the data, the excitation signal is a chirp,  $\epsilon(t)$ , described by [Eq. (7)] where  $A_1$ ,  $A_2$ ,  $P_a$ ,  $P$ ,  $t_p$ ,  $f_1$ , and  $f_2$  are constants which define amplitude, amplitude change rate, frequency change rate, total length of the chirp, and frequency range of the chirp, respectively. For the excitation used in the experiments presented in this paper, those values are:  $A_1 = 1$ ,  $A_2 = 0.25$ ,  $P_a = 0.15$ ,  $P = 0.75$ ,  $t_p = 3.596$  s,  $f_1 = 30$  Hz, and  $f_2 = 2$  kHz. The signal is quiescent for 0.5 s for a total duration of 4.096 s.

A chirp signal is used since it is a more effective signal for building up a sufficient signal to noise ratio.<sup>13</sup> After collecting the data,  $U(\mathbf{r}, t)$ , the chirp signal is removed via deconvolution and the data is convolved with a differentiated Gaussian pulse yielding  $D(\mathbf{r}, t)$ . This exchange of the chirp signal for the differentiated Gaussian pulse is best described mathematically in the frequency domain [Eq. (8)], where  $\mathcal{F}$  and  $\mathcal{F}^{-1}$  are the standard Fourier and inverse Fourier transforms, respectively.<sup>14</sup> Care should be taken that the frequency range of the Gaussian pulse is chosen to be within

the frequency range of the initial chirp signal such that the pulse contains useful information over the entire frequency range of interest,

$$\gamma(t) = (t - t_d) \exp\left(\frac{(t - t_d)^2}{\tau_w}\right), \quad (5)$$

$$\tau_w = \frac{\sqrt{2}}{\omega_c}, \quad (6)$$

$$\epsilon(t) = \left\{ A_1 + \left[ (A_2 - A_1) \frac{t}{t_p} \right]^{P_a} \right\} \times \sin \left\{ t(2\pi) \left[ f_1 + \left( \frac{f_2 - f_1}{p + 1} \right) \left( \frac{t}{t_p} \right)^p \right] \right\}, \quad (7)$$

$$D(\mathbf{r}, t) = \mathcal{F}^{-1} \left\{ \frac{\mathcal{F}\{U(\mathbf{r}, t)\}}{\mathcal{F}\{\epsilon(t)\}} \mathcal{F}\{\gamma(t)\} \right\}. \quad (8)$$

*Uniform excitation:* All sources are excited with identical differentiated Gaussian pulses. This excitation method is simple to create, and requires no *a priori* knowledge of the physical characteristics of the medium. In the presence of clutter, the wave front may be scattered, reducing the uniformity of the excitation throughout the medium.

*Time-delayed focusing:* Here the pulses are time-delayed such that all pulses arrive at a focus location at the same time. Ideally, this method focuses energy to a specific point, creating a larger excitation at the focal point, but this effect is sensitive to variations in wave propagation speed. Calculation of the time-delays for each pulse requires knowledge of the propagation speed throughout the entire medium. Propagation speeds can be affected by the presence of inhomogeneity. When the Rayleigh wave speed is known, along with the distance from source  $S_n$  to the target, the time delays can be calculated such that all the pulses arrive at the same time.

*Time-reversal focusing:* Separate measurements are performed in which a pulse is propagated from one of the sources, recorded at the focal point and then time-reversed ( $t \Rightarrow -t$ ). The time-reversed signals are then transmitted from their corresponding source locations (Fig. 2). Unlike time-delayed focusing, time-reversal requires no knowledge of the propagation speed in the medium.

## IV. EXPERIMENTAL SETUP

The experimental results are obtained in a laboratory at the Georgia Institute of Technology (Fig. 3).<sup>1</sup> A large concrete wedge-shaped tank is filled with approximately 50 tons of damp compacted sand. Sand is chosen as the background medium because its seismic properties are similar to many types of soil, and because it is straightforward to recondition disturbed sand. This allows for easy burial and removal of scattering objects and targets in the tank.

The seismic waves are generated by an array of 12 electrodynamic shakers. A short metal bar foot is attached to each electrodynamic shaker. The shaker and metal foot are placed in contact with the sand and the 12.5 cm  $\times$  1.27 cm  $\times$  2.54 cm aluminum bar foot couples seismic energy into the sand.

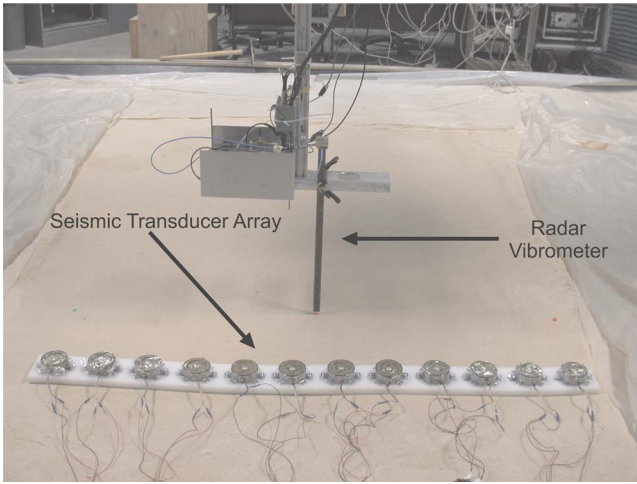


FIG. 3. (Color online) The experimental facility. The seismic transducer array and the antenna are positioned over the sand tank.

Once the shakers are used to excite elastic waves in the sand tank, a noncontact electromagnetic sensor (radar vibrometer) is used to record the displacement of the surface of the ground. The vibrometer is scanned across the surface of the sand using a computer controlled positioning system. The surface is sampled at 2 cm increments ( $\Delta x = \Delta y = 2$  cm) over a  $1.2 \text{ m} \times 0.8 \text{ m}$  area. The radar has a spot size of approximately  $2 \text{ cm} \times 2 \text{ cm}$  and records data at each location for 4.096 s at a sampling rate of 8 kHz. By making many measurements, each at a different location on the surface, the displacement of the entire scan region can be constructed synthetically. After the entire scan has been completed, a data array of displacement information is available,  $D(x_i, y_j, t_k)$ , where

$$x_i = i\Delta x, \quad i = 0, 1, \dots, \frac{X \text{ cm}}{\Delta x}$$

$$y_j = j\Delta y, \quad j = 0, 1, \dots, \frac{Y \text{ cm}}{\Delta y}, \quad (9)$$

$$t_k = k\Delta t, \quad k = 0, 1, \dots, \frac{T}{\Delta t}$$

and where  $X$  and  $Y$  are the dimensions of the scan region and  $T$  is the duration of time for which each measurement is recorded.

The theoretical development of time-reversal focusing using a TRM assumes that all sources and receivers are infinitesimally small points. In the physical experiment, the sources are distributed due to their use of a foot to couple energy into the ground. Similarly, the receivers are also distributed since the smallest resolvable area is limited by the spot size of the radar. While these distributed elements represent a deviation from the theoretical development of time-reversal using a TRM, the time-reversal method developed in Sec. III is insensitive to this change. Empirical observations demonstrate that the effectiveness of time-reversal focusing is not impacted by the use of distributed sources and receivers.



FIG. 4. (Color online) The layout of the rocks before being buried below the surface.

A total of 113 rocks are buried in the sand tank (Fig. 4) in order to introduce inhomogeneities into the sand. The rocks are randomly distributed throughout the tank both in location on the surface and burial depth. The burial region extends far beyond the scan region; rocks are buried to within 0.5 m of the edges of the sand tank. The maximum burial depth of the top of any rock is limited to approximately 20 cm. The size of the rocks varies from 10 cm in diameter to approximately 35 cm in diameter (Fig. 5).

## V. WIENER FILTER

In order to effectively illuminate a buried target using time-reversal focusing, the excitation pulse that reaches the target should be both broadband and compact in time. In addition to being useful for time-reversal focusing, a compact pulse allows for better separation of incident pulses and those reflected off a target. This separation is important for affiliated detection techniques such as time-reversal imaging.<sup>15,16</sup>

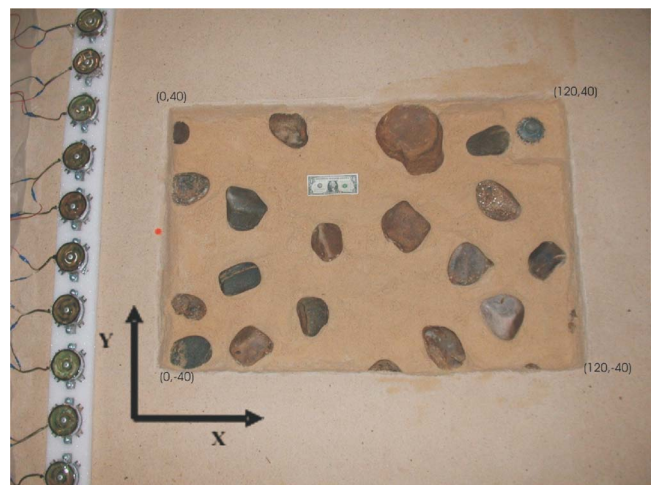


FIG. 5. (Color online) The scan region has been excavated to show the final buried rock distribution. The TS-50 landmine and the dollar bill are for scale.

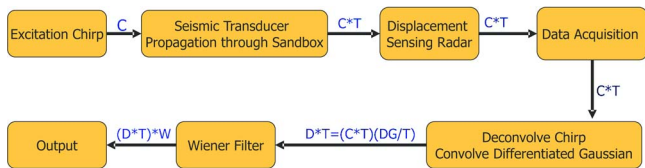


FIG. 6. (Color online) Flow graph showing the effect on the signal of its propagation through the experimental system.

In order to excite elastic waves in the ground, an excitation signal is formed digitally, passed through a D/A converter, a power amplifier, and into the electrodynamic shaker. The shaker foot then couples the transducer motion into the sand, and the excitation signal propagates through the sand and interacts with objects buried in the tank (Fig. 6). The transfer function of the electrodynamic shaker and the coupling of the shaker foot to the ground modify the excitation signal from its original temporal shape and frequency content such that the signal that arrives at the target location in the medium is significantly different from the electrical signal which is transmitted to the seismic transducer. The other elements in the signal path (A/D, amplifier, etc.) have a negligible effect on modification of the signal. The most dramatic alteration of the original excitation signal is caused by the coupling between the shaker and the ground. In the case of time-reversal focusing, this effect is more pronounced because the signal passes through the system twice, doubling the effect of the shaker-ground coupling.

To achieve the best results from time-reversal focusing, it is important to ensure that the pulse that arrives at the target is broadband and temporally compact. The practical way to do this is to design an inverse filter to restore the original response of the excitation signal. The propagating wave in the sand contains several different wave types, but the one of principal interest in the detection of buried targets is the Rayleigh surface wave. In order to most effectively design a filter that makes the Rayleigh wave temporally compact and broadband, a signal processing technique<sup>17</sup> is used to extract the Rayleigh wave mode from the total propagating wave.

A Wiener filter is designed that conditions the observed Rayleigh wave mode excitation signal resulting in a filtered excitation signal that is very similar to the desired temporally compact, broadband excitation pulse. A post-emphasis filter implementation is chosen because of the slightly nonlinear nature of the coupling between the shaker foot and the ground. A pre-emphasis filter would excite large amplitude displacements of the seismic transducer, which would drive the sand into an undesired nonlinear response. The recorded signal remains above the noise floor over the entire frequency range of interest, thereby making the post-emphasis filter an acceptable filter implementation scheme.

The filter coefficients are determined by recording signal outputs in an uncluttered medium, and extracting the Rayleigh wave mode. This information is used to design the Wiener filter using the Stieglitz-McBride method. The Stieglitz-McBride method iteratively minimizes the difference between the desired and designed filter impulse responses for computation of the optimal least-mean-square

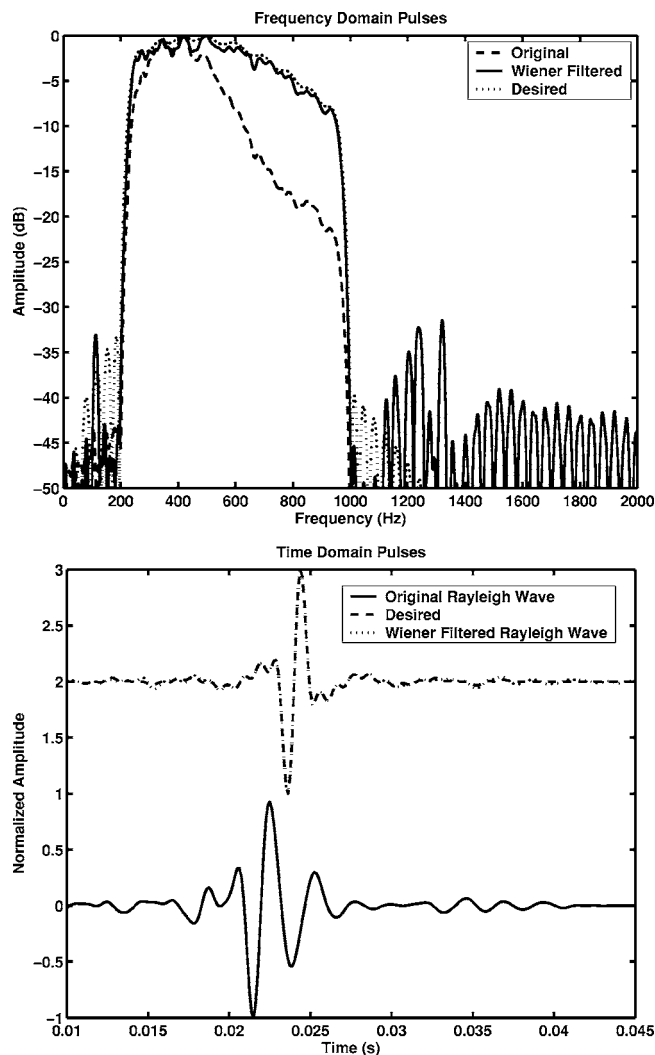


FIG. 7. Wiener filter design. (a) Frequency domain responses. (b) Time domain responses.

filter coefficients.<sup>18</sup> The frequency and time-domain responses of the unfiltered excitation signal, the desired signal, and the Wiener-filtered signal are displayed in Fig. 7.

## VI. EXPERIMENTAL RESULTS

Focusing results for all three excitation methods are first presented for a focus location near the center of the scan region. Subsequently, three additional focusing locations are chosen. These particular locations are deliberately chosen in order to examine the relative effectiveness of time-reversal focusing when it is impeded by scattering, or very near or far from the source array. Time-reversal focusing is also used to illuminate a TS-50 landmine in two of these locations. The results of this excitation are compared to the results when the transducer array is uniformly excited.

The first results to be presented (Fig. 8) are time snapshot images comparing the effectiveness of the different focusing methods for a location near the center of the scan region. These images are formed by considering the displacement array,  $D(x, y, t)$  [Eq. (9)] at a particular time. The results are presented as pseudo-color graphs of the magnitude of the vertical component of the particle displacement at

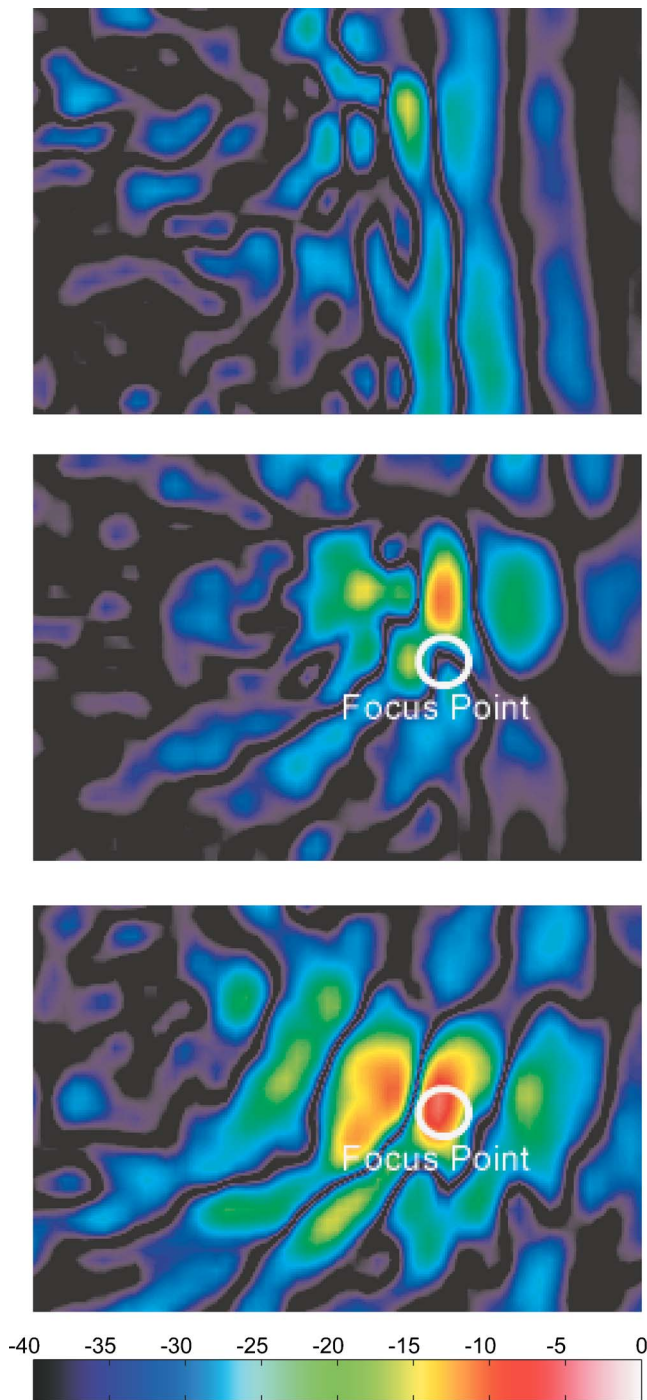


FIG. 8. (Color online) Time-snapshots for Focus Point 1. Images are on a 40 dB pseudo-color scale: 0 dB (white) to -40 dB (black). (a) Uniform excitation. (b) Time-delayed excitation. (c) Time-reversed excitation. (d) Color-amplitude scale.

the surface. The pseudo-color scale used in the viewgraphs is a 40 dB logarithmic scale from white (0 dB) to black (-40 dB). The images are normalized such that the excitation signals for each method have equal energy in the frequency band of interest,  $200 \text{ Hz} < f < 1 \text{ kHz}$ .

The first case is uniform excitation of the transducer array [Fig. 8(a)]. An excitation pulse is launched from the source array, located to the left of the scan region. As the pulse propagates through the cluttered scan region, the wave fronts are broken up by the scattering objects in the medium.

An excitation pulse not modified by scattering would appear as a set of parallel, straight wave fronts propagating away from the sources. Observation of the provided time snapshot for the uniform excitation case demonstrates that the wave fronts are significantly altered by the scattering objects.

For the time-delayed excitation, an attempt is made to focus to a point near the center of the scan region, indicated by the label, *Focus Point* [Fig. 8(b)]. The speed of the Rayleigh wave is estimated from the uniform excitation experiment and used to calculate the appropriate time delays. In this case, the time-delayed focusing attempt misses the desired focus point. The most likely reason for this is the propagation velocity gradient across the surface of the tank. Due to the gradient in the direction normal to the propagation direction, the wave front moves faster on one side than the other, causing asymmetrical arrival at the focus point. A second factor is the proximity of the desired focal location to a large rock. This rock also alters the propagation speed and path of the pulses. The cumulative effect of these conditions is that the components from each of the sources add coherently, but in the wrong location.

An examination of an attempt to focus on the same location using time-reversal focusing demonstrates significant improvement over the time-delayed focusing case [Fig. 8(c)]. The time-reversal focusing method is relatively insensitive to propagation velocity gradients and the presence of inhomogeneities in the medium. This indicates that time-reversal offers a distinct advantage in focusing when the propagation medium contains unknown variations in the propagation speed, and un-catalogued scattering objects.

A second method of presenting the results from Fig. 8, is shown in Fig. 9. This presentation of the data displays the maximum displacement at each location over the entire time record. This image is formed by creating and displaying the array,  $M(x, y)$  where

$$M(x_i, y_i) = \max_k |D(x_i, y_i, t_k)|. \quad (10)$$

The results are presented as pseudo-color graphs of the magnitude of the vertical component of the particle displacement at the surface. The pseudo-color scale used in the viewgraphs is a 40 dB logarithmic scale from white (0 dB) to black (-40 dB).

The scattering effects of rocks and other objects are visible in the uniform excitation case [Fig. 9(a)]. There are also areas of the scan region that are not effectively excited by the pulse, which will be referred to as shadow regions. An examination of the time-delayed excitation graph [Fig. 9(b)], shows that it focuses energy to a small area near the desired excitation point, but not on top of it. As discussed previously, this is due to propagation velocity gradients in the medium, and the presence of scattering objects. In a highly cluttered and inhomogeneous environment, time-delayed focusing fails to excite the focus point effectively. This makes time-delayed focusing excitation only marginally useful for detection of near surface targets in the presence of large scale clutter and inhomogeneity.

The time-reversal focusing result [Fig. 9(c)] is qualitatively similar to the time-delayed excitation focusing graph.

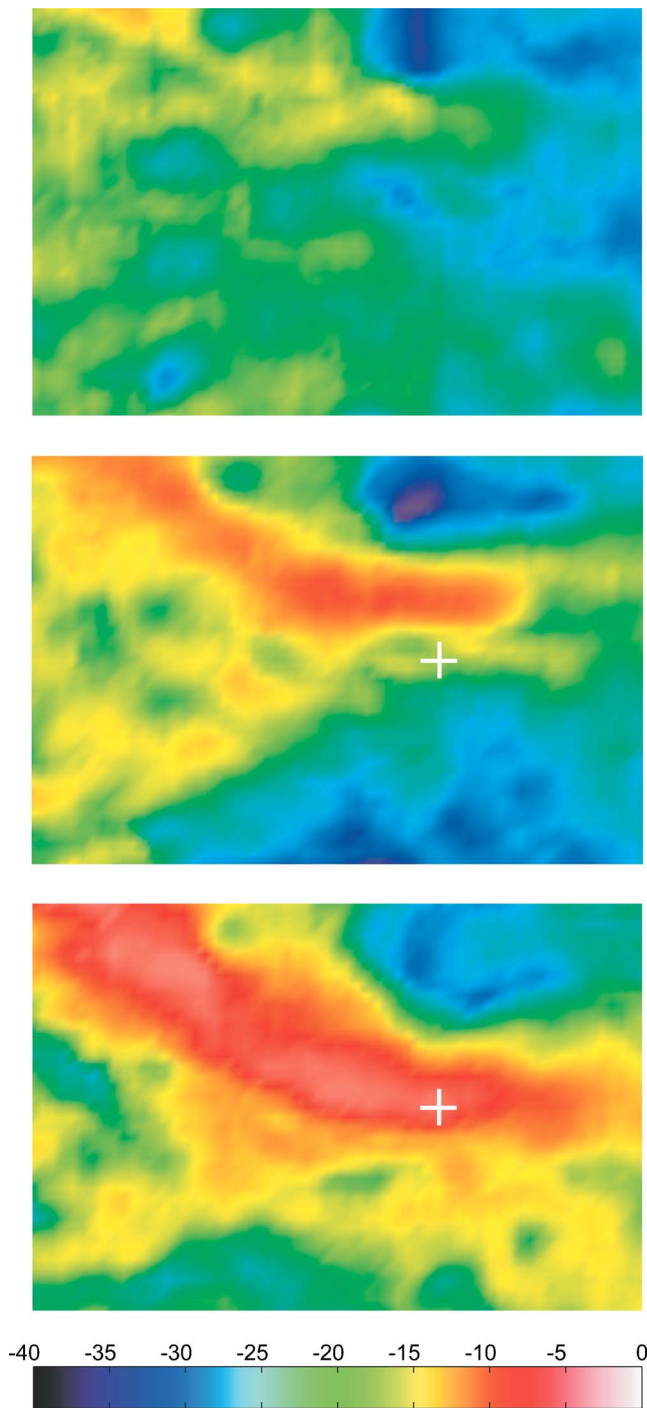


FIG. 9. (Color online) Maximum displacement for Focus Point 1. Images are on a 40 dB pseudo-color scale: 0 dB (white) to  $-40$  dB (black). The desired focusing location is indicated by a white cross. (a) Uniform excitation. (b) Time-delayed excitation. (c) Time-reversed excitation. (d) Color-amplitude scale.

A notable exception is that the maximum displacement occurs at the desired focus point in the time-reversal case. The reason for this improvement is that the time-reversal method inherently incorporates the effects of scatterers and variations in propagation velocity when calculating the time-reversed excitation pulse. It should also be noted that the displacement at the focus point is much larger than the displacement throughout the rest of the medium. This means

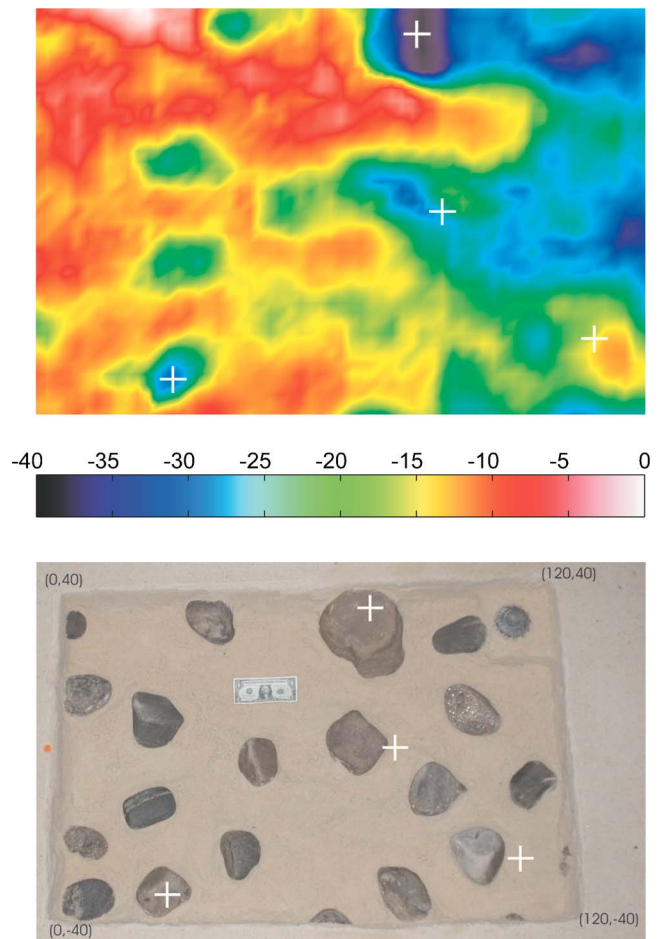


FIG. 10. (Color online) Focusing locations. (a) Uniform excitation — maximum displacement. Locations chosen for focusing are indicated by white crosses. The image is presented on a 20 dB pseudo-color scale: 0 dB (white) to  $-20$  dB (black). (b) Color-amplitude scale. (c) Layout of rocks in experimental setup. Locations chosen for focusing are indicated by white crosses.

that the interaction of the excitation pulse with the scattering objects has been significantly reduced in comparison to the uniform excitation case.

In the above-presented results, it is clear that time-reversal focusing yields significant advantages over the other excitation methods in the presence of clutter and variations in wave speed. To further investigate the effectiveness of time-reversal focusing in other circumstances, the time-reversal focusing method is applied to several new locations. These locations are selected by examining the maximum displacement graph for the uniform excitation experiment (Fig. 10). Two locations are chosen that are in shadow regions, where very little energy arrives. A third point is chosen that is far from the source, with a relatively high level of excitation. By examining this location, it is possible to study the improvement afforded by time-reversal when signal levels are already high at the desired focus point.

It has already been demonstrated (Figs. 8 and 9) that time reversal can be an effective method of excitation in regions that are poorly illuminated by traditional excitation methods. The first point chosen [Fig. 11(a)] attempts to focus energy on top of a large rock. Time-reversal increases the excitation level at the desired point, but appears to focus in

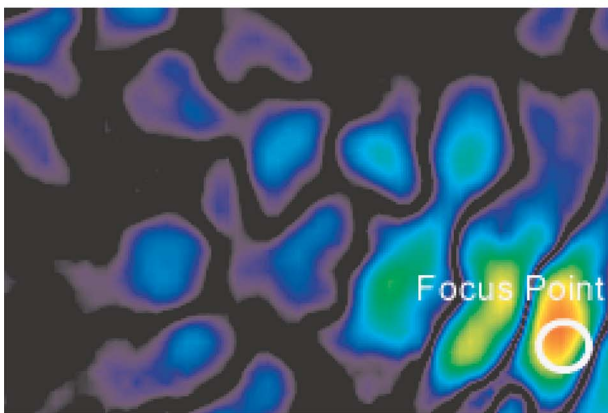
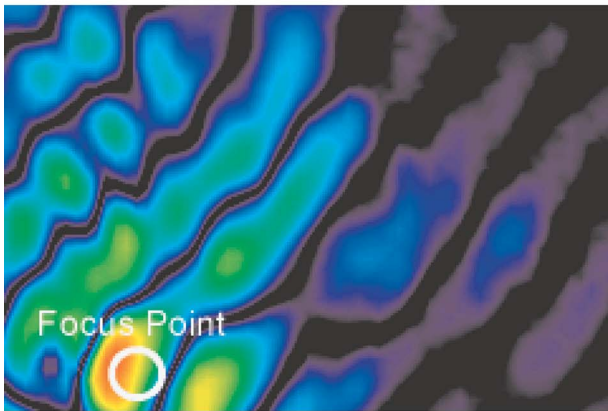
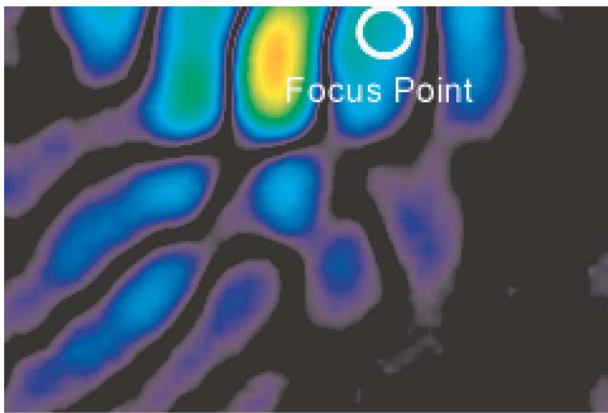


FIG. 11. (Color online) Time-reversal excitation. The desired focus point is indicated in each image. Images are on a 40 dB pseudo-color scale: 0 dB (white) to  $-40$  dB (black). (a) Shadow region: focus point 1. (b) Shadow region: focus point 2. (c) Normal excitation region focus point.

front of the rock. In the second shadow-region focus location, similar results are observed [Fig. 11(b)]. The primary difference in this case is that the actual focus location is closer to the desired one, and the excitation level is higher.

The results presented in Fig. 8(a) measure a snapshot of displacement at a particular time. These images do not take into account the varying impedance of the materials present in the sand tank. In the case of Fig. 8(a), time-reversal appears to miss the focus point and focus in front of the desired location. If this image were a measure of energy, one would be able to account for the greatly increased stiffness of the rock present at the desired focus point and demonstrate that the time-reversal signal does in fact focus significant energy to the desired location.

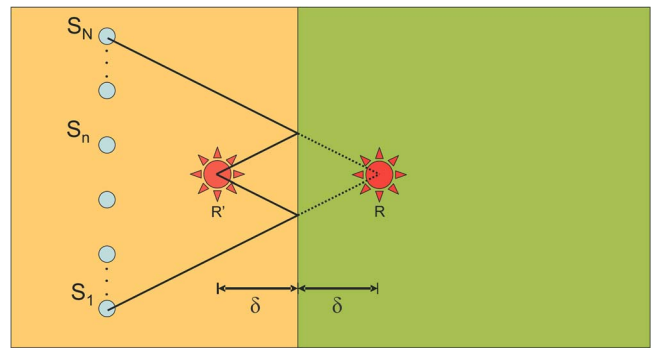


FIG. 12. (Color online) The pseudo-focus point ( $R'$ ) created by an infinite half-space rock.

The explanation above accounts for the absence of significant displacements at the focus point. The observation of a large apparent focus between the source array and the desired focus point can be described using a simple model. For the coordinate system assumed in these experiments, consider a rock of an arbitrary thickness in  $X$ , but of infinite extent in  $Y$  and  $Z$  (Fig. 12). As the wave propagating from each of the sources arrives at the medium interface, the majority of the energy in the Rayleigh wave will be reflected off the interface between the rock and the sand. This creates a pseudo-focal point,  $R'$ , in front of the rock-soil interface. In this simple case,  $R'$  will be the same distance ( $\delta$ ) away from the interface as the desired focus,  $R$ .

In the actual, less simplistic case, as the extent of the rock becomes finite, a larger portion of the incident wave is unaffected by the abrupt change in material properties. Combining this with inhomogeneities in the medium causes variation in the strength, size, and location of the pseudo-focal point. These effects are apparent when comparing Figs. 11(a) and 11(b). In the former, where the scattering rock is larger in the  $Y$  dimension (Fig. 10), a more distinct pseudo-focus point is apparent. This indicates that more of the incident waves are partially reflected and refocus in front of the desired focus location. This effect is diminished for Fig. 11(b), where the scattering rock is significantly smaller.

In the final case [Fig. 11(c)], time-reversal focuses almost exactly at the desired location and some improvement in the excitation level is observed in comparison to the uniform excitation case. The small offset of the actual focus point from the desired focus point can be attributed to the phenomenon discussed above and described in Fig. 12.

The motivation for pursuing high excitation levels at a specified location is to excite greater resonances in a landmine buried at the focus location. To that end, the effect of time-reversal on resonance excitation in a landmine is presented. Two locations are chosen, one of which is in a shadow region.

For each point, the maximum displacement level over time is used as a basis for performance comparison. For the focus location in a shadow region (Fig. 13), time-reversal focusing provides an approximately 18 dB improvement over the uniform excitation case. In addition to raising the relative amplitude of the displacement at the location of the

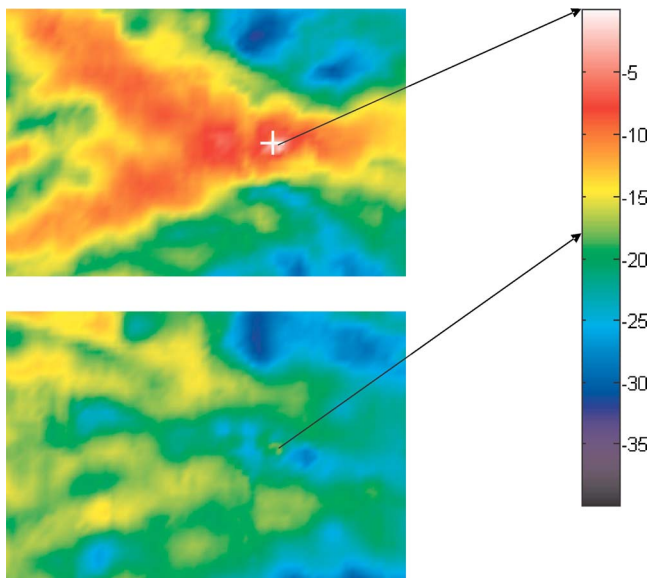


FIG. 13. (Color online) A comparison of the maximum displacement at the location of a buried TS-50 for time-reversal and uniform excitation cases.

mine, the relative signal levels over the majority of the scan region are reduced significantly, providing better contrast between the landmine and its background.

In the second position (Fig. 14), the displacement levels are high enough in the uniform excitation case to excite a substantial resonance in the landmine. While time-reversal focusing does focus energy to the location of the landmine and drop the relative displacement in the background, the increase in the displacement at the location of the resonating landmine is somewhat less, at approximately 12 dB.

## VII. CONCLUSIONS

Time-reversal behavior in an elastic medium has been examined with particular interest in its application to the problem of seismic landmine detection. In the context of the

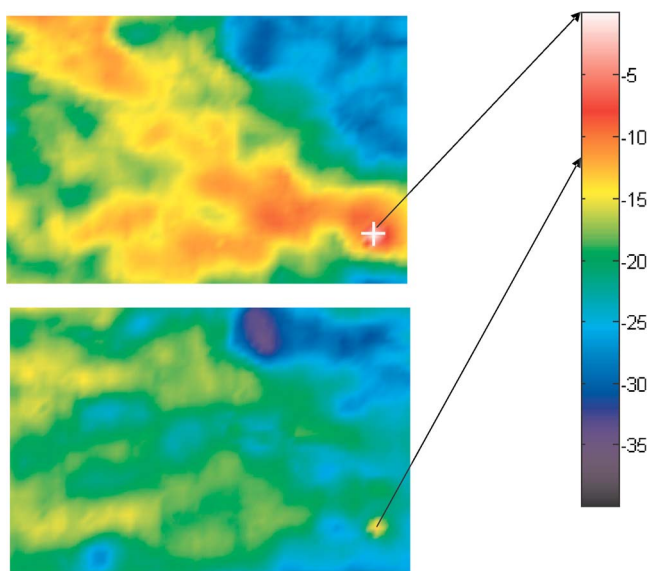


FIG. 14. (Color online) A comparison of the maximum displacement at the location of a buried TS-50 for time-reversal and uniform excitation cases.

detection system, an implementation of time-reversal focusing and a method for ensuring broadband excitation signals were developed and implemented.

Attempts were made to focus energy into various regions of interest including shadow regions and regions where signal levels were already high. An explanation was offered for the reason time-reversal focusing appears to miss its target focal point in some of these cases. The excitation of a resonance in a TS-50 landmine was compared for time reversal and uniform excitation methods.

The experimental results for time-reversal in an inhomogeneous medium at the frequency range of interest are consistent with the theoretically predicted behavior. Time-reversal has been demonstrated to be a superior excitation under certain conditions, but it has also been observed that there are situations in which time-reversal may not yield the expected result in a complex environment (Fig. 11). The conditions under which time-reversal shows the most dramatic improvement over other focusing methods are when a strong wave speed gradient is present in the medium, normal to the direction of propagation. The specific advantage of time-reversal over other methods is that time-reversal requires no *a priori* knowledge of the characteristics of the background medium.

The potential and limitations of time-reversal should continue to be investigated in future work. Super-resolution effects were not apparent in these experiments. Further studies might look to classify more specifically what the effect is of various types, configurations, and sizes of scattering objects on the effectiveness of time-reversal focusing, and under what conditions super-resolution effects can be expected to occur.

## ACKNOWLEDGMENTS

The authors would like to thank Dr. Gregg D. Larson for his assistance in designing the LABVIEW code for the experimental measurements and Dr. James H. McClellan and Mubashir Alam for their assistance in designing the Wiener filter.

- <sup>1</sup>W. R. Scott Jr., J. S. Martin, and G. D. Larson, "Experimental model for a seismic landmine detection system," *IEEE Trans. Geosci. Remote Sens.* **39**, 1155–1164 (2001).
- <sup>2</sup>M. Fink, "Time-reversal of ultrasonic fields. i. Basic principles," *IEEE Trans. Ultrason. Ferroelectr. Freq. Control* **39**, 555–556 (1992).
- <sup>3</sup>F. Wu, J.-L. Thomas, and M. Fink, "Time-reversal of ultrasonic fields. ii. Experimental results," *IEEE Trans. Ultrason. Ferroelectr. Freq. Control* **39**(5), 567–578 (1992).
- <sup>4</sup>D. Cassereau and M. Fink, "Time-reversal of ultrasonic fields. iii. Theory of the closed time-reversal cavity," *IEEE Trans. Ultrason. Ferroelectr. Freq. Control* **39**, 579–592 (1992).
- <sup>5</sup>A. Derode, P. Roux, and M. Fink, "Robust acoustic time reversal with high-order multiple scattering," *Phys. Rev. Lett.* **75**, 4206–4209 (1995).
- <sup>6</sup>M. Fink, C. Prada, F. Wu, and D. Cassereau, "Self focusing in inhomogeneous media with time reversal acoustic mirrors," *IEEE Ultrason. Symp.* **2**, 681–686 (1989).
- <sup>7</sup>P. Blomgren, G. Papanicolaou, and H. Zhao, "Super-resolution in time-reversal acoustics," *J. Acoust. Soc. Am.* **111**, 230–248 (2002).
- <sup>8</sup>L. Borcea, G. Papanicolaou, and C. Tsogka, "Theory and applications of time reversal and interferometric imaging," *Inverse Probl.* **19**(6), 139–164 (2003).
- <sup>9</sup>P. D. Norville, W. R. Scott Jr., and G. D. Larson, "An investigation of time reversal techniques in seismic landmine detection," *Proc. SPIE* **5415**,

1310–1322 (2004).

- <sup>10</sup>R. Ing, M. Fink, and O. Casula, “Self-focusing rayleigh wave using a time reversal mirror,” *Appl. Phys. Lett.* **68**, 161–163 (1996).
- <sup>11</sup>J.-L. Thomas, F. Wu, and M. Fink, “Self focusing on extended objects with time reversal mirror, applications to lithotripsy,” *IEEE Ultrason. Symp.* **3**, 1809-1814 (1993).
- <sup>12</sup>D. C. Carsten Draeger and M. Fink, “Theory of time-reversal process in solids,” *J. Acoust. Soc. Am.* **102**, 1289–1295 (1997).
- <sup>13</sup>J. S. Martin, W. R. Scott Jr., G. D. Larson, P. H. Rogers, and G. S. M. II, “Probing signal design for seismic landmine detection,” *Proc. SPIE* **5415**, 133–144 (2004).
- <sup>14</sup>R. N. Bracewell, *The Fourier Transform and Its Applications*, 3rd ed. (McGraw-Hill, New York, NY, 2000).
- <sup>15</sup>M. Alam and J. H. McClellan, “Near field imaging of subsurface targets using active arrays and elastic waves,” *IEEE Digital Signal Processing Workshop*, 2004.
- <sup>16</sup>M. Alam, J. H. McClellan, P. D. Norville, and W. R. Scott, Jr., “Time-reverse imaging for the detection of landmines,” *Proc. SPIE* **5415**, 167–174 (2004).
- <sup>17</sup>M. Alam, J. H. McClellan, and W. R. Scott Jr., “Multi-channel spectrum analysis of surface waves,” *37th Asilomar Conference on Signals, Systems and Computers*, 2003.
- <sup>18</sup>K. Steiglitz and L. McBride, “A technique for the identification of linear systems,” *IEEE Trans. Autom. Control* **AC-10**, 461–464 (1965).